Environment, Development and Sustainability (2020) 22:4145–4167
https://doi.org/10.1007/s10668-019-00376-7

Enhancement of potable water production from an inclined photovoltaic panel absorber solar still by integrating with flat-plate collector

A. Muthu Manokar[1] · M. Vimala[2] · Ravishankar Sathyamurthy[3,4] · A. E. Kabeel[4] · D. Prince Winston[5] · Ali J. Chamkha[6]

Received: 26 December 2018 / Accepted: 11 May 2019 / Published online: 18 May 2019

Abstract

This manuscript brings out with an enhancement of the freshwater productivity from the active inclined solar panel basin solar still (AISPBSS). The research was conducted on the AISPBSS by the diversified mass flow rate of water (m_f). The maximum freshwater yield obtained at m_f at 1.8, 3.2 and 4.7 kg/h is 7.5, 6.5 and 5.4 kg, respectively. The daily average thermal and exergy efficiency of the AISPBSS at m_f at 1.8, 3.2 and 4.7 kg/h is 43.71, 38.27 and 29.62% and 8.39, 6.94 and 5.08%, respectively. The daily average PV panel power production of 47.71, 49.84 and 53.83 watts, electrical efficiency of 7.2, 7.6 and 8.1%, thermal efficiency of 17.3, 18.3 and 19.7%, exergy efficiency of 18.32, 20.23 and 22.39%, the overall thermal efficiency of 61.39, 57.44 and 51.37% and the overall exergy efficiency of 26.52, 27.14 and 27.40% are obtained from the system under m_f at 1.8, 3.2 and 4.7 kg/h, respectively. When m_f increases, there are decreases in the AISPBSS distillate yield, thermal, exergy and the overall thermal efficiency and increases in the PV panel power production and electrical, thermal, exergy and the overall exergy efficiency. Further, energy return term and carbon credit attained for the AISPBSS have been calculated. It was found that payback period of 20, 18.7 and 17.5 years and carbon credit earned of 21, 25 and 30 $ are obtained at m_f at 1.8, 3.2 and 4.7 kg/h, respectively.

Keywords Photovoltaic panel-integrated solar still · Mass flow rates · Panel efficiency · PV thermal and exergy analysis · Energy payback period · Carbon credit earned

Abbreviations

CSS	Conventional solar still
EHTC	Evaporative heat transfer coefficient
EPBP	Energy payback period
AISPBSS	Active inclined solar panel basin solar still
ISS	Inclined solar still
IWSS	Inclined wick solar still
PSS	Pyramid solar still

✉ Ravishankar Sathyamurthy
raviannauniv23@gmail.com; ravishankars05@outlook.com

Extended author information available on the last page of the article

PV	Photovoltaic
SSS	Stepped solar still
VFPR	Vertical flat-plate reflector

List of symbols

A	Area (m^2)
A	Area of solar panel (m^2)
CO_2	Carbon dioxide
E	Energy (kWh)
E_{in}	Embodied energy (kWh)
E_{out}	Annual energy output (kWh)
Exinput	Exergy input of solar still (W/m^2)
Exoutput	Exergy output of solar still (W/m^2)
H	Monthly average irradiation on PV panels
h	Heat transfer coefficient (W/m^2K)
I	Current (A)
I (t)	Solar intensity (W/m^2)
L	Life of the system (years)
L_{fg}	Latent heat of vaporization (kJ/kg K)
m_{ew}	Hourly productivity from solar still (kg/m^2 h)
m_f	Mass flow rate (kg/h)
P	Power production
PR	Performance ratio, coefficient for losses (range between 0.9 and 0.5, default value = 0.75)
PV	Photovoltaic
PV/T	Photovoltaic/thermal
r	Solar panel efficiency (%)
T	Temperature (°C)
V	Voltage (V)
$\eta_{overall,exe}$	Overall exergy effectiveness (%)
η_{pv}	Solar panel effectiveness (%)

Subscript

a	Ambient
d	Daily
e	Evaporation
g	Glass
s	Sun
w	Water

1 Introduction

Over the earlier time, shortage of potable water has turned out to be progressively risky due to the regularly expanding populace of the world, the fast improvement in an industry and the increasing contamination of water assets. Close to 2025, there will be the significant issue confronting half of the total populace, to be specific the absence of the freshwater (Kabeel et al. 2018). Elective methods for producing the potable water must be found. A lot of studies have been done to augment the freshwater from the solar still. Among the several design modifications (single-basin, double-basin, single-slope and double-slope solar still, pyramid, tubular and hybrid solar still), inclined solar still (ISS) performance is better than the conventional solar still (CSS). The main advantage of an ISS over the CSS is, it can maintain minimum water depth of the basin. A slim layer of water in the absorber plate results in quick evaporation and higher yield than the CSS (Kabeel et al. 2017). El-Agouz et al. (2015) theoretically examined the ISS performance by reusing the hot water to the still basin using the water pump. Aybar et al. (2016) carried out the comparative investigation of single-basin ISS and double-basin ISS. Ravishankar et al. theoretically (Sathyamurthy et al. 2016) and experimentally (Nagarajan et al. 2017) calculated the production rate of the ISS with and without baffle plates by varying m_f. The freshwater production from the ISS with and without baffles was 5.4 and 3.4 kg/m^2, respectively. El-Agouz (2014) used a storage tank for continuous water circulation in a stepped solar still (SSS) to augment the production time. He found that SSS with saltwater as inlet formed the daily productivity of 6.3 L/m^2 and seawater formed the productivity of 6.1 L/m^2. Comparative study of the CSS and the SSS with reflectors attached to the perpendicular sides of the steps was done by Omara et al. (2013). The SSS with and without an internal reflector improves the daily yield of about 75 and 57%, respectively, than the CSS. Omara et al. (2014) also researched the SSS with internal mirrors and outside mirrors (top and bottom). This system produced the maximum yield of about 8100 ml/m^2 which was 125% higher than the CSS. Velmurugan et al. (2009) researched the SSS for sewage desalination. It was found that the productivity of the SSS with fins, with fins and pebbles, with fins and sponge and with fins, pebbles and sponge was 1.27, 1.37, 1.4 and 1.65 L/m^2, respectively. The freshwater production rate was increased about 53, 68, 65 and 98% when fins, fins and pebbles, fins and sponge and fins, pebbles and sponge, respectively. Abujazar et al. (2017a, b) researched the SSS performance by replacing an absorber plate made of galvanized iron tray with copper tray. The absorber plate was made of copper to increase the thermal conductivity of the absorber plate. This SSS enhances the evaporation area of about 55.6% more than the CSS. It was found that copper inclined SSS produced the daily maximum freshwater production of about 4383 ML/m^2 and maximum hourly efficiency of 58% at 5 p.m. Tanaka and Nakatake (2007) introduced the novel vertical flat-plate reflector (VFPR) attached inclined wick solar still (IWSS) and numerically derived its performance. In this system, wick-type absorber plate received the direct, diffuse and reflected solar intensity. It was found that an IWSS with and without VFPR produces the daily maximum yield of about 6.5 and 5.7 kg/m^2, respectively. Tanaka (2011, 2013) also numerically studied the performance of the bottom flat-plate reflector attached with an IWSS. It was found that an IWSS with and without bottom flat-plate reflector produces the daily maximum yield of about 7.5 and 6.01 kg/m^2, respectively. Sathyamurthy et al. (2015) introduced a novel semicircular trough basin solar still coupled with baffles. Experiments were conducted by m_f at 8 kg/h and 10 number of baffles arranged in an absorber plate and results were compared with the CSS. It was concluded that the novel system with baffles and the CSS provide the maximal yield of 3.2 and 2.6 kg/m^2 and maximum efficiency of 38.48 and 32.4%, respectively. Experimental study of pyramid solar still (PSS) integrated with an ISS with baffles has been done by Kumar et al. (2017). In this research, three solar stills (PSS, ISS and PSS integrated with ISS) were tested. Experiments were conducted by the ISS at m_f at 8.33 kg/h and the PSS at water height of 0.02, 0.04 and 0.06 m, respectively. The daily productivity from the PSS, ISS and PSS integrated with the ISS is 4.2, 5.04 and 7.52 kg/m^2, respectively. Economic and exergy analysis of the PSS and the PSS integrated with an ISS with baffles has been done by Panchal et al. (2017). From the exergy analysis, it was reported that exergy efficiency during the evening time was higher for the 0.05-m water depth. The maximum exergy efficiency of 14 and 35% was obtained for the PSS and still integration at the higher water depth.

Different experimental works were conducted on the PV panel integrated with an FPC in the active type solar distillation, and it was submitted that this system produced the water productivity of 6–10 kg/m^2/day. By integrating the solar panel in the still, the productivity was increased about 60% than the CSS (Kumar and Tiwari 2009, 2010; Dev and Tiwari 2010; Gaur and Tiwari 2010; Kumar 2013; Eltawil and Omara 2014; Saeedi et al. 2015; Tiwari et al. 2015; Singh et al. 2016). Kabeel et al. (2012) researched the CSS by incorporating with the rotary fan which was operated by a vertical shaft powered by the PV panel. It was submitted that this system produced the daily productivity of 4.75 L/m^2 and it was 25% higher than the CSS. The solar still incorporated with the vacuum tube coupled with a PV panel has been experimentally investigated by Abdallah et al. (2009). Yari et al. (2016) researched the active type solar still by attaching the solar cells at the glass surface, and it was reported that this system produced 32% higher productivity than the CSS. Hidouria et al. (2017) and Al-Nimr et al. (2016) developed a hybrid desalination system. The CSS integrated with an AC heater and a solar panel was experimentally studied by Riahi et al. (2015) and Praveen Kumar et al. (2017).

Abdullah (2013) has done the design modifications of SSS such as the use of aluminum filling in the absorber plate as thermal storage medium, integrating solar air heater (active mode) and glass cover cooling technology. Kabeel et al. (2012) researched the SSS performance by varying the width of trays, depth of water, attaching a wick cloth on the perpendicular side of the trays and an integrating the vacuum tube solar collector (active mode).

Al-Nimr and Qananba (2018) researched a novel CSS incorporated with a finned condensing unit, solar cells and thermoelectric generator. Experiments were conducted on hybrid system with and without condensing unit. From the experimentation, it was reported that distilled water production rate increased up to 27% when ambient temperature increased from 10 to 35 °C and solar intensity was 1000 W/m^2 and production rate decreased up to 37% when the wind velocity was 10 m/s. Similarly, finned condensing unit increased the distilled water production rate up to 14% as compared to the CSS. This hybrid system negatively affects the solar cells performance for the reasons of higher heat gain in the PV cells. Fathy et al. (2018) fabricated parabolic trough collector (PTC) integrated with a double-slope solar still (DSSS). In this work, oil pipes are connected with a solar still basin to transmit heat from the PTC to the DSSS. Experiments were conducted on CSS, CSS integrated with fixed PTC and CSS integrated with tracked PTC at the water depth of 20 and 30 mm, respectively. It was submitted that the maximum daily yield of 4.51, 8.53 and 10.93 kg/m^2 and daily efficiency of 36.87, 23.26 and 29.81% were obtained for the CSS, CSS integrated with fixed PTC and CSS integrated with tracked PTC, respectively, at 20 mm water depth on summer month. The CSS integrated with tracked PTC produced 142.3% higher freshwater production than the CSS. Malaeb et al. (2016) numerically derived the performance of the modified solar still with and without rotating drum in the basin of the still. It was reported that still with rotating drum produced about 3 L of water whereas still without rotating drum produced about 1 L of water. Singh et al. (2016) researched the CSS and DSSS performance by using energy matrices based on exergy for the atmospheric conditions of India. It was reported that based on the exergy analysis CSS performance is better than the DSSS. Singh and Tiwari (2017a) theoretically augmented the DSSS energy matrices by integrating with N identical PVT collector. It was reported that hybrid PVT integrating with the FPC coupled with DSSS produced higher annual yield than the hybrid PVT integrating with the CPC coupled with DSSS and conventional DSSS. Singh and Tiwari (2017b) also numerically derived the performance of the CSS and DSSS by integrating with PVT-CPC. It was reported that DSSS performance was higher than the CSS.

Al-Nimr et al. (2018) researched a distiller with photovoltaic/thermoelectric cooler (PV/TEC). The TEC is used to augment the condensation rate and avoid excessive heating in this model. Al-Nimr and Al-Ammari (2016) also researched a new model of PV/T distillation unit with the CSS in which the solar cells were attached in the basin which produced yield of 6.8 L/m^2/day. Al-Nimr (2015) next designed a novel PV/T system, which was fitted with an evaporator and a condenser to improve its performance. Manokar et al. (2018d) introduced a PV/T-integrated ISS. In this research work, the PV panel is integrated with an ISS to produce an electrical power and freshwater. It consists of the PV panel as an absorber plate, glass collector cover and water storage tank. Water is uniformly distributed through the PVC pipe which is attached at the top of the experimental setup. Constantly water is flowing over the PV panel, which absorbs the heat energy from the panel and produces simultaneously hot water and freshwater. Increasing m_f positively affects the panel performance and negatively affects the still performance. It was submitted that increases in the basin temperature result in higher distillate yield and lower power production. The maximum productivity of 7.3 kg and efficiency of 71.2% are obtained when the system is fully insulated condition. From the above studies, it is found that only few researchers carried out an inclined solar still integrated with preheating methodologies (active mode) (Kumar et al. 2017; Abdullah 2013; Kabeel et al. 2012).

2 Identification of knowledge gap

Various comprehensive review articles have been studied (Kumar et al. 2015; Manokar et al. 2014, 2018a, b, c, 2019; Nayi and Modi 2018; Murugavel et al. 2013; Kaviti et al. 2016; Kabeel et al. 2019). From the review articles of Kali et al. (Murugavel et al. 2013), Kaviti et al. (2016) and Kabeel et al. (2019), it was found that only few experimental works have been published on active ISS. In the previous study, Manokar et al. (2018d, e) reported that bottom insulation reduces the PV panel performance because of higher panel temperature whereas without insulation reduces the freshwater yield. Hence, the main novelty of this research work is integrating the ISPB still without any insulation with an FPC to enhance the electrical performance of the solar panel and also freshwater yield.

3 Design and construction of the AISPBSS

The schematic representation and photographic view of an AISPBSS are shown in Figs. 1 and 2, respectively. The saltwater from the cylindrical water storage tank is fed into the FPC at a constant m_f. The water flowing inside the absorber tube of the FPC gets heated, and heated water is again fed into the AISPBSS. In the absorber of the AISPBSS, wick material (cotton thread) is fixed in-between the space between the solar cells to augment the evaporation rate. Due to inclined position of PV panel, water is flowing through it and hot water is collected at the bottom of the experimental setup. Every hour the collected hot water is manually filled in the storage tank. The collector cover of the experimental setup is made of 4-mm-thick normal glass. In the collector cover surface, a glass strip is attached to collect the freshwater and it is collected at the bottom of the experimental setup. m_f is adjusted by using the control valves. Thermocouples were attached at the different places of the experimental setup to measure the temperatures. The dimensions of the FPC water heater and an AISPBSS are given in Table 1. The AISPBSS was placed at south direction with a decline equal to 13°N. During the

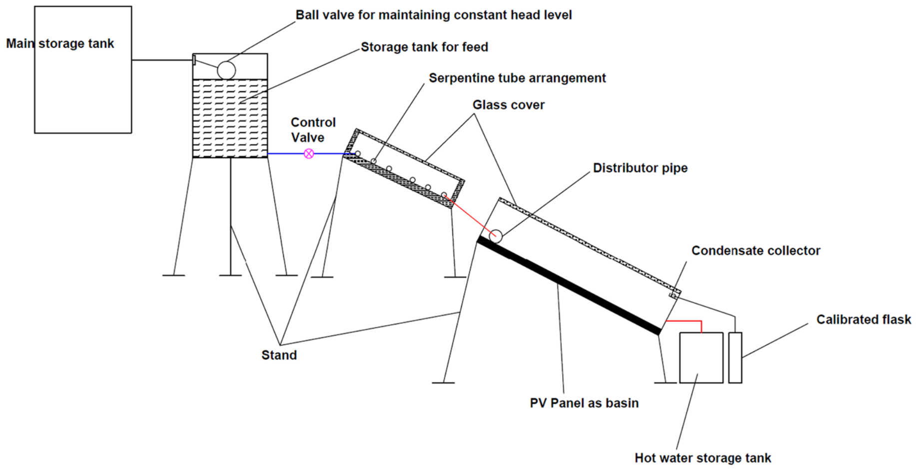

Fig. 1 Schematic diagram of an AISPBSS

Fig. 2 Photographic view of an AISPBSS

Table 1 Dimensions of an FPC water heater and AISPBSS

	Length (mm)	Width (mm)	Height (mm)
AISPBSS	1810	920	150
FPC solar water heater	900	600	200

operation of an AISPBSS, we are facing the problem of salt deposition on the solar panel and it requires maintenance. The periodic maintenance of the solar panel by Windex crystal rain glass cleaner is required because of salt deposition (Manokar et al. 2018e).

Table 2 Accuracy, range and error limits for different measuring instruments

S. no.	Instruments	Measuring parameter	Accuracy	Range
1	Thermocouple	Temperature	± 1 °C	0–100 °C
2	Solar power meter	Solar intensity	± 1 W/m^2	0–2500 W/m^2
3	Anemometer	Wind velocity	± 0.1 m/s	0–15 m/s
4	Measuring jar	Water mass	± 10 m L	0–1000 m L
5	Multimeter	Voltage and current	± 1 V	0–1000 V
			± 0.1 A	0–10 A

Table 3 Cost analysis for an AISPBSS

S. no.	Materials	Unit cost ($)	Total cost ($)
1	Solar PV panel (150 watts)	$ 1.48/watts	$ 222.68
2	Glass material (walls and collector)	$ 23.75	$ 23.75
3	Distillate collector	$1.48	$1.48
	ISPB still	(A)	$ 247.91
4	Copper material	$ 10.39	$ 10.39
5	FPC collector cover	$ 4.45	$ 4.45
6	Wooden box	$ 8.91	$ 8.91
	FPC water heater	(B)	$ 23.75
7	Storage tank and stand	$7.42	$ 7.42
8	Control valve	$ 2.23/2 pieces	$ 4.45
9	Windex crystal rain glass cleaner	$ 19.30	$ 19.30
10	Labor cost	$ 3.71/h	$ 14.85
	Accessories and labor cost	(C)	$ 46.02
	Total cost	(A + B + C)	$ 317.68

1$ = Rs 67.39

The range and accuracy in the present investigations are given in Table 2. The detailed error analysis of the instrument (uncertainty) is provided in "Appendix." Cost breakdown for the AISPBSS is given in Table 3.

Experiments were performed on July 2017 in three different m_f conditions: (i) 1.8, (ii) 3.2 and (iii) 4.7 kg/h. During the testing period, the average solar intensity was calculated and three similar atmospheric conditions days July 21, 2017 (average I(t) 718 W/m^2), July 23, 2017 (average I(t) 709 W/m^2), and July 24, 2017 (average I(t) 716 W/m^2), were selected for the comparative studies.

4 Results and discussion

4.1 Variations of solar irradiance, wind speed, atmospheric temperature and glass temperature

Fluctuations of the solar irradiance and atmosphere temperature for the duration of the study of an AISPBSS are shown in Fig. 3a, b. During the testing periods, the solar intensity

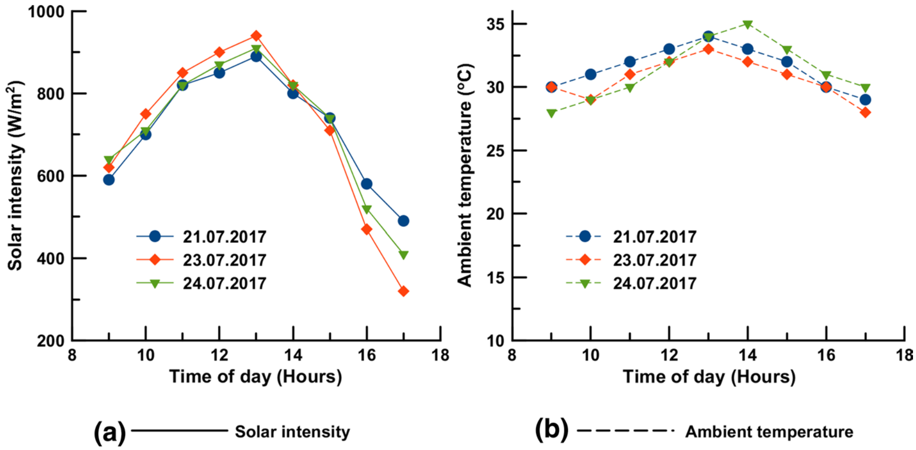

Fig. 3 Diurnal variation of **a** solar intensity and **b** atmospheric temperature

and atmosphere temperature increase at the morning session and attained its highest value at 1 p.m. At the evening session, it is decreasing. The maximum solar intensity of 890, 940 and 910 W/m^2 and the daily average solar intensity of 718, 709 and 716 W/m^2 are noted on July 21, 2017, July 23, 2017, and July 24, 2017, respectively. The maximum atmosphere temperature of 34, 33 and 35 °C is noted on July 21, 2017, July 23, 2017, and July 24, 2017, respectively. During the experimental day, the daily average atmospheric temperature is between 30 and 32 °C.

Variations of wind speed and the collector cover temperature during the study of an AISPBSS are plotted in Fig. 4a, b. During the investigational day, the average wind speed is noted as 1.5, 1.8 and 2 m/s on July 21, 2017, July 23, 2017, and July 24, 2017, respectively. The maximum collector cover temperature of the AISPBSS is 51, 48 and 47 °C on July 21, 2017, July 23, 2017, and July 24, 2017, respectively. The daily average collector cover temperature of 45, 43 and 41.22 °C is measured for the daily average wind speed of 1.5, 1.8 and 2 m/s, respectively. From the above data, it is clear that when the wind speed is higher, collector cover surface enhances the convective heat transfer from the collector cover to the atmosphere, which resulted in lower collector cover temperature.

4.2 Effect of m_f on basin and water temperature

Variations of the basin temperature for an AISPBSS under different m_f are plotted in Fig. 5a. Basin temperature increases with increasing solar intensity and reached its peak value at 2 p.m., and from there on it gets reduced. The maximum basin temperature of 71, 67 and 65 °C is obtained for m_f at 1.8, 3.2 and 4.7 kg/h, respectively. The daily average basin temperature of an AISPBSS at m_f at 1.8, 3.2 and 4.7 kg/h is 60.78, 57.34 and 54.56 °C, respectively. When m_f increases from 1.8 to 3.2 kg/h and from 1.8 to 4.7 kg/h, there is a decrease in the daily average basin temperature of about 5.66 and 10.24%, respectively. An increase in m_f results in higher volume of flowing saline water in the AISPBSS basin, which resulted in the lower basin temperature.

Variations of the water temperature for an AISPBSS under different m_f are plotted in Fig. 5b. Water temperature is directly equivalent to the basin temperature and it reached the

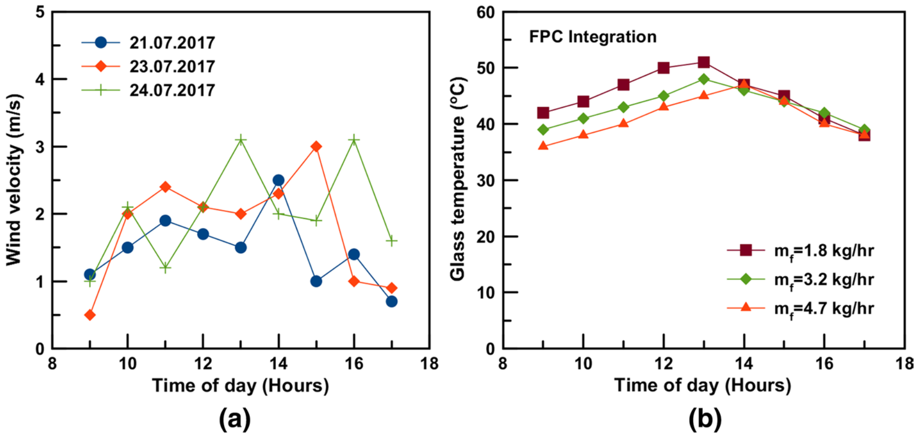

Fig. 4 Diurnal variations of **a** wind speed and **b** glass temperature

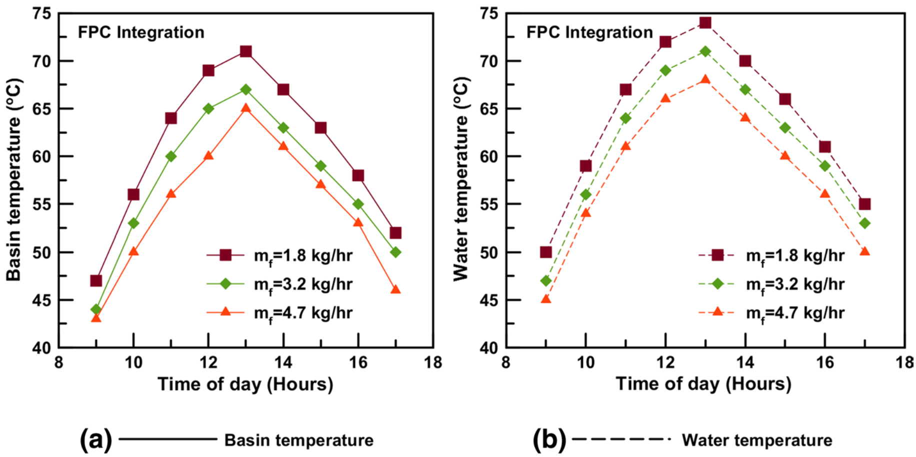

Fig. 5 Hourly variations of **a** basin temperature and **b** water temperature for an AISPBSS

peak value at 2 p.m., and from there on it gets reduced. The maximum water temperature of an AISPBSS at m_f at 1.8, 3.2 and 4.7 kg/h is 74, 71 and 68 °C, respectively. The daily average water temperature of 63.78, 61 and 58.23 °C is obtained for m_f at 1.8, 3.2 and 4.7 kg/h, respectively. Water temperature is reduced up to 4.36 and 8.71% when m_f increases from 1.8 to 3.2 kg/h and from 1.8 to 4.7 kg/h, respectively. The minimum m_f of an AISPBSS increases the contact time between the saline water and the absorber plate, which resulted in higher water temperature and hence higher yield. m_f is inversely proportional to the basin and water temperature. When m_f increases, the volume of flowing water in the absorber plate increases, which reduces the contact time between the saline water and an absorber plate and hence produces lower productivity.

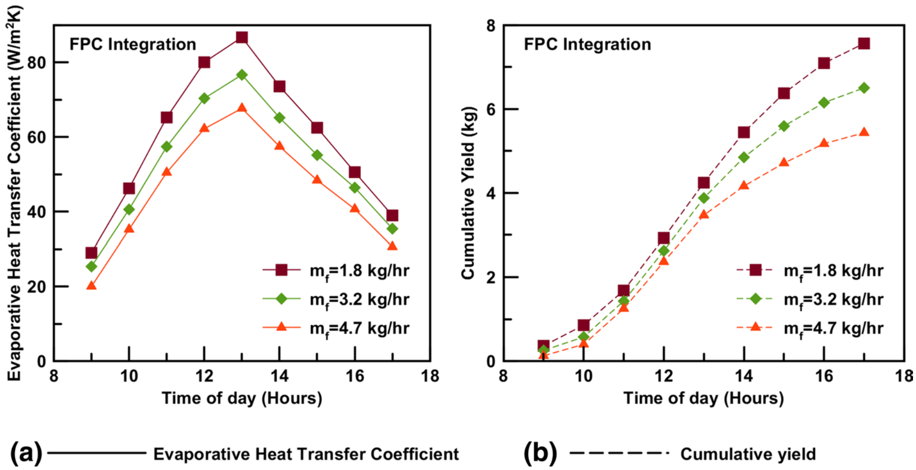

Fig. 6 Hourly variations of **a** EHTC and **b** accumulated yield for an AISPBSS

4.3 Effect of m_f on Evaporative Heat Transfer Coefficient (EHTC), accumulated yield, thermal and exergy efficiency

Variations of the EHTC for an AISPBSS at different m_f are shown in Fig. 6a. The maximum EHTC of 86.7, 76.7 and 67.6 W/m^{2}k is obtained for an AISPBSS under m_f at 1.8, 3.2 and 4.7 kg/h, respectively. The daily average EHTC for an AISPBSS under m_f at 1.8, 3.2 and 4.7 kg/h is 59.2, 52.5 and 45.86 W/m^{2}k, respectively. There are 11.31 and 22.53% decreases in daily average EHTC when m_f is increased from 1.8 to 3.2 kg/h and from 1.8 to 4.7 kg/h, respectively. An increase in m_f decreased the saline water temperature and EHTC, hence resulted in lower freshwater production.

The EHTC from the feed water to glass is calculated by (Manokar et al. 2018d),

$$h_{e,w-g} = 16.273 \times 10^{-3} x h_{c,w-g} \left[\frac{P_w - P_{gi}}{T_w - T_{gi}} \right] \tag{1}$$

The convective heat transfer coefficient from the feed water to glass is calculated by (Manokar et al. 2018d),

$$h_{c,w-g} = 0.884 \left[\left(T_w - T_{gi}\right) + \frac{\left(P_w - P_{gi}\right)\left(T_w + 273\right)}{\left(268.9 \times 10^{-3} - P_w\right)} \right] \tag{2}$$

Partial vapor pressure at the feed water temperature and inner glass is calculated by (Manokar et al. 2018d),

$$P_w = \exp\left(25.317 - \left(\frac{5144}{273 + T_w}\right)\right) \tag{3}$$

$$P_{gi} = \exp\left(25.317 - \left(\frac{5144}{273 + T_{gi}}\right)\right) \tag{4}$$

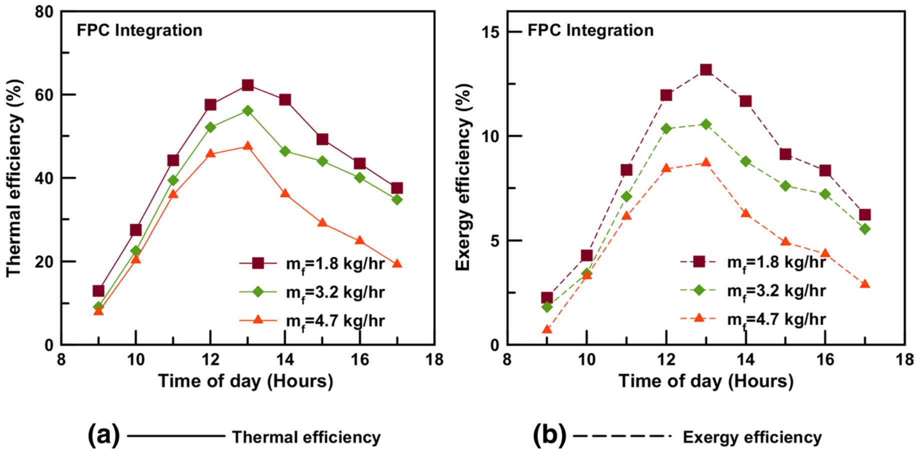

Fig. 7 Hourly variations of **a** thermal efficiency and **b** exergy efficiency for an AISPBSS

Variations of cumulative yield for an AISPBSS at different m_f are shown in Fig. 6b. The daily productivity from an AISPBSS is maximum at minimum m_f. The daily productivity from an AISPBSS at m_f at 1.8, 3.2 and 4.7 kg/h is 7.5, 6.5 and 5.4 kg, respectively. The amount of distilled yield production from the AISPBSS mainly depends on the water temperature. It can be seen that at the minimum m_f, the basin water temperature is higher. It is found that the daily yield decreases up to 14 and 28.14% when m_f increases from 1.8 to 3.2 kg/h and from 1.8 to 4.7 kg/h, respectively.

Variations of thermal efficiency for an AISPBSS at different m_f are plotted in Fig. 7a. The highest thermal efficiency for an AISPBSS at m_f at 1.8, 3.2 and 4.7 kg/h is 62.24, 56.11 and 47.5%, respectively. It is found 43.71, 38.27 and 29.62% of daily average thermal efficiency for an AISPBSS at m_f at 1.8, 3.2 and 4.7 kg/h, respectively. The thermal efficiency of an AISPBSS is decreased when m_f is increased. There are 12.45 and 32.24% decreases in the daily average thermal efficiency of an AISPBSS when m_f is increased from 1.8 to 3.2 kg/h and from 1.8 to 4.7 kg/h, respectively.

Thermal effectiveness of the AISPBSS is given by (Manokar et al. 2018e),

$$\eta_{A.th} = \frac{m_{ew} h_{fg}}{\left[A_c \times I_c(t) + A_s \times I_s(t)\right] \times 3600} \times 100 \tag{5}$$

Variations of the exergy efficiency for an AISPBSS under different m_f are shown in Fig. 7b. The maximum hourly exergy efficiency of an AISPBSS is 13.2, 10.6 and 8.7% at m_f at 1.8, 3.2 and 4.7 kg/h, respectively. The daily average exergy efficiency of 8.39, 6.94 and 5.07% is obtained for m_f at 1.8, 3.2 and 4.7 kg/h, respectively. An increase in m_f resulted in decreasing exergy efficiency of the AISPBSS. When m_f is increased from 1.8 to 3.2 kg/h and from 1.8 to 4.7 kg/h, the exergy efficiency of an AISPBSS decreased up to 17.3 and 39.4%, respectively. Table 4 summarizes the positive outputs of productivity, energy efficiency and exergy efficiency by decreasing m_f in an AISPBSS.

The exergy efficiency of the AISPBSS is given by (Manokar et al. 2018e),

$$\eta_{a.e} = \frac{e_{a.out}}{e_{p.in} + e_{fpc.in}} \tag{6}$$

Table 4 Improvements in yield and the energy and exergy efficiency of the AISPBSS for different m_f

S. no	Mass flow rate (kg/h)	Yield (kg)		Energy efficiency (%)		Exergy efficiency (%)	
		Actual	% Increase	Actual	% Increase	Actual	% Increase
1	4.7	5.4	Reference	29.62	Reference	5.07	Reference
2	3.2	6.5	17	38.27	22.6	6.94	27
3	1.8	7.5	28	43.71	32.2	8.39	39.6

The exergy output of the AISPBSS is given by (Manokar et al. 2018e),

$$e_{a.out} = \left(m_d x h_{fg}\right)\left(1 - \left[\frac{T_a + 273}{T_w + 273}\right]\right) \tag{7}$$

The exergy input of the AISPBSS is given by (Manokar et al. 2018e),

$$e_{a.in} = e_{p.in} + e_{fpc.in} \tag{8}$$

The exergy input to the solar water heater is given by (Manokar et al. 2018e),

$$e_{fpc.in} = Q_u\left[1 - \frac{T_a + 273}{T_w + 273}\right] \tag{9}$$

The heat attained by the solar water heater is given by (Manokar et al. 2018e),

$$Q_u = \left(IxA_p\right) - q \tag{10}$$

The heat lost from the solar water heater is given by (Manokar et al. 2018e),

$$q = UA\left(T_b - T_a\right) \tag{11}$$

4.4 Effect of m_f on the solar panel power production, solar panel electrical, energy and exergy efficiency of the AISPBSS

Figure 8a–d shows the deviation of the solar panel temperature and solar panel efficiencies for an AISPBSS at different m_f. From Fig. 8a–d, it is noted that the panel temperature decreases with an increase in m_f. The PV panel temperature reached the maximum value of 63, 59 and 54 °C for m_f at 1.8, 3.2 and 4.7 kg/h, respectively. The daily average panel temperature at m_f at 1.8, 3.2 and 4.7 kg/h is 51.34, 49 and 44.56 °C, respectively. An increase in m_f resulted in decreases in panel temperature. The daily average panel temperature decreases up to 4.55 and 13.2% when m_f increases from 1.8 to 3.2 kg/h and from 1.8 to 4.7 kg/h, respectively.

It is noted that the maximum hourly PV panel power generation and efficiency from an AISPBSS at m_f at 1.8, 3.2 and 4.7 kg/h are 70.2, 74.1 and 80 watts and 8.6, 8.9 and 9.6%, respectively. Similarly, the daily average power generation and efficiency are 46, 50.88 and 55.16 watts and 7.13, 7.62 and 8.14% for m_f at 1.8, 3.2 and 4.7 kg/h, respectively. The power generation from an AISPBSS is increased with increasing m_f. It is found that there are 4.2 and 5.2% increases in the PV panel power production and the efficiency when the daily average PV panel temperature reduces up to 4.55%. Similarly, there are 11.4 and 12% increases in the PV panel power production and the efficiency when the daily average PV panel temperature reduces up to 13.2%.

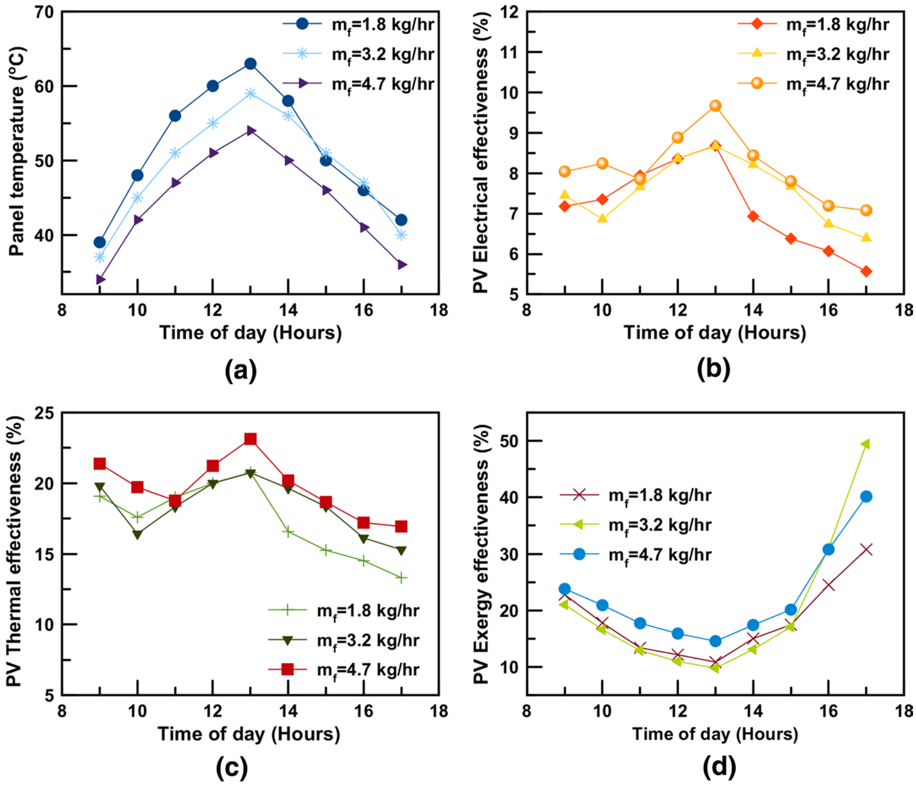

Fig. 8 Hourly variations of **a** solar panel temperature, **b** PV electrical efficiency, **c** PV thermal effectiveness and **d** PV exergy effectiveness for the different flow rates (m_f)

The electrical efficiency of the PV panel is calculated by (Manokar et al. 2018e),

$$\eta_{\text{pv electrical}} = \frac{FF \times V \times I}{I_s(t) \times A_s} \times 100\% \quad (12)$$

The thermal efficiency of the PV panel has the same trend as the solar panel electrical efficiency and it reached its maximal value of 20.76, 20.74 and 23.13% at m_f at 1.8, 3.2 and 4.7 kg/h, respectively. The daily average thermal efficiency of the solar panel is 17.34, 18.30 and 19.69% at m_f at 1.8, 3.2 and 4.7 kg/h, respectively.

The thermal efficiency of the solar panel is obtained by (Singh et al. 2016),

$$\eta_{\text{pv thermal}} = \frac{FF \times V_{oc} \times I_{sc}}{0.38 I_s(t) \times A_s} \times 100\% \quad (13)$$

Figure 8a–c shows that the exergy efficiency of the PV panel is maximum at the minimum panel temperature. The daily average solar panel exergy efficiency is 18.32, 20.23 and 22.39% at m_f at 1.8, 3.2 and 4.7 kg/h, respectively. When m_f is increased from 1.8 to 3.2 kg/h and from 1.8 to 4.7 kg/h, the exergy efficiency of a PV panel increases up to 9.5 and 18.2%, respectively.

The exergy efficiency of the solar panel is calculated by (Singh et al. 2016),

Table 5 Improvements in the PV panel power generation and efficiency of the AISPBSS for different m_f

S. no	Mass flow rate (kg/h)	PV panel power (watts)		PV panel efficiency (%)	
		Actual	% Increase	Actual	% Increase
1	1.8	46	Reference	7.13	Reference
2	3.2	50.88	9.6	7.62	6.4
3	4.7	55.16	16.6	8.14	12.4

$$\eta_{\text{pv exergy}} = \frac{FF \times V_{oc} \times I_{sc} - VI}{0.933 I_s(t) \times A_s} \times 100\% \quad (14)$$

Table 5 shows the improvements made in the PV panel power production and efficiency by increasing m_f in an AISPBSS.

4.5 Monthly power generation from the system at different m_f

The monthly solar radiation data for the experimental place are obtained from the Atmospheric Science Data Center, NASA Surface Meteorology and Solar Energy—location[1]

Monthly power generated from the solar panel is theoretically calculated by the following formula,[2]

$$E = A \times r \times H \times \text{PR} \quad (15)$$

Table 6 shows the monthly power generation from the PV panel at different flow rates. From the table, it is identified that the electrical power production from the solar panel is maximum on March month and minimum on November month for the average monthly solar intensity of 205.84 and 121.5 kWh, respectively. The annual electrical energy generation from the PV panel at m_f at 1.8, 3.2 and 4.7 kg/h is 101.96, 108.96 and 116.4 kWh, respectively. The annual energy generation from the panel at m_f at 3.2 and 4.7 kg/h is 6.43 and 12.41% higher than the minimum m_f.

4.6 Environmental analysis

4.6.1 Embodied energy (E_{in})

Total embodied energy is the total energy necessary to manufacture the AISPBSS (Eltawil et al. 2018; Saini et al. 2017). The embodied energy of the different components which are used in the present study is given in Table 7.

4.6.2 Energy payback period (EPBP)

EPBP is the entire period essential to recover the total E_{in} involved in manufacturing the system. It is defined as the ratio between the E_{in} and E_{out} (Eltawil et al. 2018; Saini et al. 2017) (Table 8).

1 https://eosweb.larc.nasa.gov/cgi-bin/sse/grid.cgi.
2 http://photovoltaic-software.com/.

Table 6 Monthly power generation from the AISPBSS at different m_f

S. no.	Month	Solar intensity (kWh/ /month)	Energy (kWh) $m_f = 1.8$ kg/h $\eta_{pv} = 7.13\%$	Energy (kWh) $m_f = 3.2$ kg/h $\eta_{pv} = 7.62\%$	Energy (kWh) $m_f = 4.7$ kg/h $\eta_{pv} = 8.14\%$
1	January	152.83	8.17	8.73	9.32
2	February	164.92	8.81	9.42	10.06
3	March	205.84	11.00	11.76	12.56
4	April	201.6	10.77	11.51	12.30
5	May	189.72	10.14	10.84	11.58
6	June	157.2	8.40	8.98	9.59
7	July	146.63	7.84	8.37	8.95
8	August	148.8	7.95	8.50	9.08
9	September	150.3	8.03	8.58	9.17
10	October	137.02	7.32	7.83	8.36
11	November	121.5	6.49	6.94	7.41
12	December	131.44	7.02	7.51	8.02
Annual energy output (E_{out})			101.96	108.96	116.40

Table 7 Embodied energy calculation data for the proposed AISPBSS

S. no.	Materials	Embodied energy (kWh/kg)	Weight (kg)	Embodied energy (kWh)
1	PV panel	1130.56 (kWh/m^2)	1.6 (m^2)	1808.896
2	Aluminum angle	43.1	0.5	21.55
3	glass	4.2	5	21
4	Copper material	11.67	2	23.34
5	Wooden box	4.2	4	16.8
6	Steel stand	7	10	70
7	Storage tank	21.44	0.2	4.288
8	PVC pipe	25	3	75
Total embodied energy (kWh)				2040.874

Table 8 Calculation data for energy payback period, net CO_2 mitigation and carbon credit earned for the AISPBSS

Mass flow rate of water	1.8 kg/h	3.2 kg/h	4.7 kg/h
Energy payback period (y)	20	18.7	17.5
Net CO_2 mitigation (t)	2.1	2.5	3
Carbon credit earned ($)	21	25	30

$$\text{EPBP} = \frac{E_{\text{in}}}{E_{\text{out}}} \tag{16}$$

4.6.3 Carbon dioxide (CO_2) emission

The average CO_2 emission for the coal-based thermal power plant is approximately 0.98 kg/kW (Singh et al. 2016; Eltawil et al. 2018; Saini et al. 2017).

$$\text{Co}_2\text{emission per year} = \frac{E_{\text{in}}}{L} \times 2.042\ \text{kg} \tag{17}$$

4.6.4 Net CO_2 mitigation

The net CO_2 mitigation for the system is given by the difference between the total CO_2 mitigation and total CO_2 (Eltawil et al. 2018; Saini et al. 2017).

$$\text{Net CO}_2\text{ mitigation} = (E_{\text{out}} \times L - E_{\text{in}}) \times 2.04\ \text{kg} \tag{18}$$

4.6.5 Carbon credit

If CO_2 discharge is being traded at 10 US$/t of CO_2 mitigation, then the carbon credit earned by the system is given by (Eltawil et al. 2018; Saini et al. 2017).

$$\text{The carbon credit earned} = \text{Net CO}_2\text{ mitigation (in t)} \times 10\ \text{US\$/t} \tag{19}$$

4.7 Variations of the overall thermal and exergy efficiency of the AISPBSS

Variations of the overall thermal efficiency of the AISPBSS (thermal efficiencies of an AISPBSS and a PV panel) at different m_f are shown in Fig. 9a. The overall thermal efficiency of the AISPBSS is maximum at minimum m_f. When m_f increases, the thermal efficiency of the AISPBSS is decreased, whereas the thermal efficiency of the PV panel is increased. The maximum hourly overall thermal efficiency of the system is 83, 72.86 and 70.64% at m_f at 1.8, 3.2 and 4.7 kg/h, respectively. The daily average overall thermal efficiency of the system is 61.39, 57.44 and 51.37% at m_f at 1.8, 3.2 and 4.7 kg/h, respectively. It is concluded that there are 6.43 and 16.33% decreases in the daily overall thermal efficiency of the system when m_f is increased from 1.8 to 3.2 kg/h and from 1.8 to 4.7 kg/h, respectively.

The overall thermal efficiency of the AISPBSS is given by (Al-Nimr 2015; Manokar et al. 2018e),

$$\eta_{\text{overallA.thermal}} = \frac{m_{\text{ew}} h_{\text{fg}}}{\left[A_c \times I_c(t) + A_s \times I_s(t)\right] \times 3600} \times 100 + \frac{FF \times V_{\text{oc}} \times I_{\text{sc}} - VI}{0.933 I_s(t) \times A_s} \times 100\% \tag{20}$$

Figure 9b shows the overall exergy efficiencies of an AISPBSS at different m_f. The daily average exergy efficiency of the AISPBSS is about 8.39, 6.94 and 5.08%, daily average PV panel exergy efficiency is about 18.32, 20.23 and 22.39% and the overall average exergy efficiency of the AISPBSS is about 26.52, 27.14 and 27.40% at m_f at 1.8, 3.2 and 4.7 kg/h, respectively. The daily average exergy efficiency of the AISPBSS decreases with an increase in m_f, whereas the daily average exergy efficiency of the solar panel is increased.

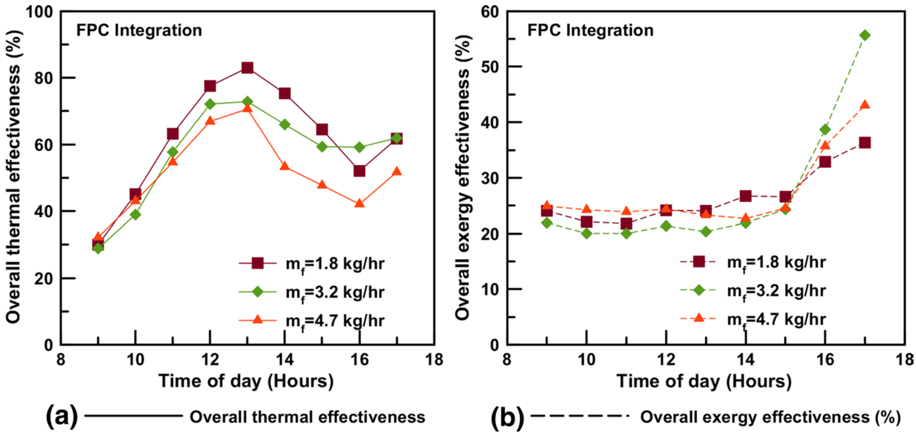

Fig. 9 Hourly variations of **a** the overall thermal and **b** the overall exergy efficiency of the AISPBSS

The reduction in exergy efficiency of the AISPBSS and increases in panel exergy efficiency resulted in nearly equal overall exergy efficiency for all m_f.

The overall exergy efficiency of the AISPBSS is given by (Al-Nimr 2015; Manokar et al. 2018e),

$$\eta_{\text{overallAexergy}} = \frac{\left(m_d \times h_{fg}\right)\left(1 - \left[\frac{T_a+273}{T_w+273}\right]\right)}{\left(A_s \times I_t\right)\left[1 + \left(\frac{1}{3}\left[\frac{T_a+273}{6000}\right]^4 - \frac{4}{3}\left[\frac{T_a+273}{6000}\right]\right)\right] + Q_u\left[1 - \frac{T_a+273}{T_w+273}\right]} + \frac{FF \times V_{oc} \times I_{sc} - VI}{0.933 I_s(t) \times A_s} \times 100\% \tag{21}$$

4.8 Comparison of yield of various types of ISS

The comparison of productivity of various types of the ISS is given in Table 9. The productivity was maximum in the case of the solar still incorporated with the electrical heater (yield—12 L/m^2) (Abdallah et al. 2009). The PV panel-integrated ISS without any insulation created the productivity of 4.4 kg (Manokar et al. 2018d). In the present study, AISPBSS produced the daily productivity of 7.5 kg. An active mode enhances the productivity up to 41.33% than the passive mode.

5 Conclusions

In drinking water and electricity scarcity region, solar still desalination is popular. Especially in desert region, government is struggling to meet the demand of drinking water and electricity. The PV panel-integrated ISS is a good option which fulfills the need of both electricity and drinking water. The results inferred that solar panel power generation mainly depends on the both panel temperature and solar intensity. In this study, the solar panel performance was improved by increasing m_f. But increasing m_f reduces the performance of an AISPBSS. When m_f is varied from 1.8 to 3.2 kg/h, the daily productivity and

Table 9 Comparison of daily yield of different types of ISS

S. no.	Author names	Type of solar still	Experimental work done	Productivity
1	El-Agouz et al. (2015)	Passive	Continuous flow ISS (Theoretical study)	7 kg
2	Aybar et al. (2016)	Passive	SB-ISS with normal absorber plate	0.85 kg/m^2/day
			SB-ISS with black-fleece wick	2.245 kg/m^2/day
			DB-ISS with normal absorber plate	1.808 kg/m^2/day
			DB-ISS with black-fleece wick	3.086 kg/m^2/day
3	Sathyamurthy et al. (2016)	Passive	ISS with baffle plates (Theoretical study)	3.5 kg/m^2
4	Nagarajan et al. (2017)	Passive	ISS with baffles	5.4 kg/m^2
			ISS without baffles	3.4 kg/m^2
5	El-Agouz (2014)	Passive	SSS with saltwater as inlet	6.3 L/m^2/day
			SSS with seawater as inlet	6.1 L/m^2/day
6	Omara et al. (2013)	Passive	SSS with reflector	6350 ml/m^2
			SSS without reflector	5840 ml/m^2
7	Omara et al. (2014)	Passive	SSS with external mirror attached on the top	6500 ml/m^2
			SSS with external mirror attached on the bottom	6830 ml/m^2
			SSS incorporated with internal and top external mirror	7400 ml/m^2
			SSS incorporated with internal and bottom external mirror	7240 ml/m^2
			SSS attached with both internal and external (top and bottom) mirrors	8100 ml/m^2
8	Velmurugan et al. (2009)	Passive	SSS with fins	1.27 L/m^2
			SSS with fins and pebbles	1.37 L/m^2
			SSS with fins and sponge	1.4 L/m^2
			SSS with fins and pebbles and sponge	1.65 L/m^2
9	Abujazar et al. (2017a, b)	Passive	Copper absorber inclined SSS	4383 ML/m^2
10	Tanaka and Nakatake (2007)	Passive	IWSS with VFPR	6.5 kg/m^2
			IWSS without VFPR	5.7 kg/m^2
11	Sathyamurthy et al. (2015)	Passive	Semicircular trough absorber solar still with baffles	3.2 kg/m^2
12	Kumar et al. (2017)	Active	PSS integrated with an ISS	7.52 kg/m^2

Table 9 (continued)

S. no.	Author names	Type of solar still	Experimental work done	Productivity
13	Kumar and Tiwari (2009, 2010), Dev and Tiwari (2010), Gaur and Tiwari (2010), Eltawil and Omara (2014), Saeedi et al. (2015) and Singh et al. (2016)	Active	Solar still with FPC integrated with PV module	6–10 kg/m^2
14	Hidouri et al. (2017)	Active	Solar still integrated with air compressor	–
15	Al-Nimr et al. (2016)	Active	Solar still integrated with wind mill	–
16	Abdullah (2013)	Active	SSS integrated with solar air heater	6300 ml/ m^2/day
17	Kabeel et al. (2012)	Active	SSS integrated with solar collector	6080 ml/ m^2/day
18	Al-Nimr and Qananba (2018)	passive	Hybrid solar still	–
19	Fathy et al. (2018)	Active	Active DSSS with fixed PTC	8.53 kg/m^2
			Active DSSS with tracked PTC	10.93 kg/m^2
20	Malaeb et al. (2016)	Passive	Solar still with rotating drum	3 L
			Solar still without rotating drum	1 L
21	Singh et al. (2016), Singh and Tiwari (2017a, b)	Active	DSSS integrated with the FPC and CPC	–
22	Al-Nimr et al. (2018), Al-Nimr and Al-Ammari (2016), Al-Nimr (2015)	Passive	PV/T distillation unit	6.8 L/m^2/day
23	Manokar et al. (2018d)	Passive	Integrating solar panel in the ISS without any insulation	4.4 kg
24	Muthu et al. (present study)	Active	AISPBSS at minimum water flow rate (present study)	7.5 kg

thermal, exergy and overall thermal efficiency of the system are decreased about 14, 12.45, 17.3 and 6.43%, respectively, and the solar panel power production and electrical, exergy and overall exergy efficiency are enhanced up to 4.3, 5.2, 9.5 and 2.29%, respectively. Further m_f is varied to 4.7 kg/h, the daily productivity and thermal, exergy and overall thermal efficiency of the system are decreased about 28.14, 32.24, 39.4 and 16.33%, respectively, and solar panel power production and electrical, exergy and overall exergy efficiency are enhanced up to 11.4, 12, 18.2 and 3.23%, respectively.

Appendix

S. no.	Instrument	Uncertainty (%)
1.	TES 1333R solar power meter	2.51
2.	AM4836 3 cup anemometer	3.32
3.	Thermocouple (RTD (PT100 type))	1.53
4.	Multimeter (voltage)	1.25
5.	Multimeter (current)	3.57
6.	Measuring jar	3.42

The uncertainty of instruments is calculated based on the internal uncertainty of instrument (U) and average values of experimental results (X). The value of U is mathematically expressed as,

$$U = \frac{\sqrt{\sigma_1^2 + \sigma_2^2 + \sigma_3^2 + \sigma_4^2 + \sigma_5^2 + \sigma_6^2 + \cdots + \sigma_n^2}}{N}$$

Similarly, the value of σ (standard deviation) is expressed as,

$$\sigma = \frac{\sqrt{\sum (X - \bar{X})}}{N}$$

The uncertainty (%) is calculated as,

$$\text{Uncertainty percentage} = \frac{U}{x} \times 100\ (\%)$$

References

Abdallah, S., Abu-Khader, M. M., & Badran, O. (2009). Performance evaluation of solar distillation using vacuum tube coupled with photovoltaic system. *Applied Solar Energy, 45*(3), 176–180.

Abdullah, A. S. (2013). Improving the performance of stepped solar still. *Desalination, 319,* 60–65.

Abujazar, M. S. S., Fatihah, S., Ibrahim, I. A., Kabeel, A. E., & Sharil, S. (2017a). Productivity modelling of a developed inclined stepped solar still system based on actual performance and using a cascaded forward neural network model. *Journal of Cleaner Production, 170,* 147–159. https://doi.org/10.1016/j.jclepro.2017.09.092.

Abujazar, M. S. S., Fatihah, S., & Kabeel, A. E. (2017b). Seawater desalination using inclined stepped solar still with copper trays in a wet tropical climate. *Desalination, 423,* 141–148.
Al-Nimr, M. A. (2015). Modeling of a novel concentrated PV/T distillation system enhanced with a porous evaporator and an internal condenser. *Solar Energy, 120,* 593–602.
Al-Nimr, M. A., & Al-Ammari, W. A. (2016). A novel hybrid PV-distillation system. *Solar Energy, 135,* 874–883.
Al-Nimr, M. D. A., Al-Ammari, W. A., & Alkhalidi, A. (2018). A novel hybrid photovoltaics/thermoelectric cooler distillation system. *International Journal of Energy Research*.
Al-Nimr, M. A., Kiwan, S. M., & Talafha, S. (2016). Hybrid solar-wind water distillation system. *Desalination, 395,* 33–40.
Al-Nimr, M. A., & Qananba, K. S. (2018). A solar hybrid system for power generation and water distillation. *Solar Energy, 171,* 92–105.
Aybar, H. Ş., Irani, F., & Arslan, M. (2016). Performance analysis of single and double basin-inclined solar water distillation systems with and without black-fleece wick. *Desalination and Water Treatment, 57*(37), 17167–17181.
Dev, R., & Tiwari, G. N. (2010). Characteristic equation of a hybrid (PV-T) active solar still. *Desalination, 254,* 126–137.
El-Agouz, S. A. (2014). Experimental investigation of stepped solar still with continuous water circulation. *Energy Conversion and Management, 86,* 186–193.
El-Agouz, S. A., El-Samadony, Y. A. F., & Kabeel, A. E. (2015). Performance evaluation of a continuous flow inclined solar still desalination system. *Energy Conversion and Management, 101,* 606–615.
Eltawil, M. A., Azam, M. M., & Alghannam, A. O. (2018). Energy analysis of hybrid solar tunnel dryer with PV system and solar collector for drying mint (MenthaViridis). *Journal of Cleaner Production*. https://doi.org/10.1016/j.jclepro.2018.01.229.
Eltawil, M. A., & Omara, Z. M. (2014). Enhancing the solar still performance using solar photovoltaic, flat plate collector and hot air. *Desalination, 349,* 1–9.
Fathy, M., Hassan, H., & Ahmed, M. S. (2018). Experimental study on the effect of coupling parabolic trough collector with double slope solar still on its performance. *Solar Energy, 163,* 54–61.
Gaur, M. K., & Tiwari, G. N. (2010). Optimization of number of collectors for integrated PV/T hybrid active solar still. *Applied Energy, 87,* 1763–1772.
Hidouria, K., Mishrab, D. R., Benhmidenea, A., & Chouachia, B. (2017). Experimental and theoretical evaluation of a hybrid solar still integrated with an air compressor using ANN. *Desalination and Water Treatment, 88,* 52–59.
Kabeel, A. E., Abdelgaied, M., & Essa, A. (2018). Enhancing the performance of single basin solar still using high thermal conductivity sensible storage materials. *Journal of Cleaner Production, 183,* 20–25. https://doi.org/10.1016/j.jclepro.2018.02.144.
Kabeel, A. E., Hamed, M. H., & Omara, Z. M. (2012a). Augmentation of the basin type solar still using photovoltaic powered turbulence system. *Desalination and Water Treatment, 48*(1–3), 182–190.
Kabeel, A. E., Khalil, A., Omara, Z. M., & Younes, M. M. (2012b). Theoretical and experimental parametric study of modified stepped solar still. *Desalination, 289,* 12–20.
Kabeel, A. E., Manokar, A. M., Sathyamurthy, R., Winston, D. P., El-Agouz, S. A., & Chamkha, A. J. (2019). A review on different design modifications employed in inclined solar still for enhancing the productivity. *Journal of Solar Energy Engineering, 141*(3), 031007.
Kabeel, A. E., Teamah, M. A., Abdelgaied, M., & Abdel Aziz, G. B. (2017). Modified pyramid solar still with v-corrugated absorber plate and PCM as a thermal storage medium. *Journal of Cleaner Production, 161,* 881–887. https://doi.org/10.1016/j.jclepro.2017.05.195.
Kaviti, A. K., Yadav, A., & Shukla, A. (2016). Inclined solar still designs: A review. *Renewable and Sustainable Energy Reviews, 54,* 429–451.
Kumar, S. (2013). Thermal–economic analysis of a hybrid photovoltaic thermal (PVT) active solar distillation system: Role of carbon credit. *Urban Climate, 5,* 112–124.
Kumar, P. N., Manokar, A. M., Madhu, B., Kabeel, A. E., Arunkumar, T., Panchal, H., et al. (2017). Experimental investigation on the effect of water mass in triangular pyramid solar still integrated to inclined solar still. *Groundwater for Sustainable Development, 5,* 229–234. https://doi.org/10.1016/j.gsd.2017.08.003.
Kumar, P. V., Kumar, A., Prakash, O., & Kaviti, A. K. (2015). Solar stills system design: A review. *Renewable and Sustainable Energy Reviews, 51,* 153–181.
Kumar, S., & Tiwari, A. (2010). Design, fabrication and performance of a hybrid photovoltaic/thermal (PV/T) active solar still. *Energy Conversion and Management, 51,* 1219–1229.
Kumar, S., & Tiwari, G. N. (2009). Estimation of internal heat transfer coefficients of a hybrid (PV/T) active solar still. *Solar Energy, 83,* 1656–1667.

Malaeb, L., Aboughali, K., & Ayoub, G. M. (2016). Modeling of a modified solar still system with enhanced productivity. *Solar Energy, 125,* 360–372.
Manokar, A. M., Murugavel, K. K., & Esakkimuthu, G. (2014). Different parameters affecting the rate of evaporation and condensation on passive solar still—A review. *Renewable and Sustainable Energy Reviews, 38,* 309–322.
Manokar, A. M., Prince Winston, D., Kabeel, A. E., Sathyamurthy, R., & Arunkumar, T. (2018a). Different parameter and technique affecting the rate of evaporation on active solar still—A review. *Heat and Mass Transfer, 54,* 593–630.
Manokar, A. M., Taamneh, Y., Kabeel, A. E., Sathyamurthy, R., Winston, D. P., & Chamkha, A. J. (2018b). Review of different methods employed in pyramidal solar still desalination to augment the yield of freshwater. *Desalination and Water Treatment, 136,* 20–30.
Manokar, A. M., Vimala, M., Winston, D. P., Ramesh, R., Sathyamurthy, R., Nagarajan, P. K., et al. (2019). Different parameters affecting the condensation rate on an active solar still—A review. *Environmental Progress & Sustainable Energy, 38*(1), 286–296.
Manokar, A. M., Winston, D. P., Kabeel, A. E., El-Agouz, S. A., Sathyamurthy, R., Arunkumar, T., et al. (2018c). Integrated PV/T solar still—A mini-review. *Desalination, 435,* 259–267.
Manokar, A. M., Winston, D. P., Kabeel, A. E., & Sathyamurthy, R. (2018d). Sustainable fresh water and power production by integrating PV panel in inclined solar still. *Journal of Cleaner Production, 172,* 2711–2719.
Manokar, A. M., Winston, D. P., Mondol, J. D., Sathyamurthy, R., Kabeel, A. E., & Panchal, H. (2018e). Comparative study of an inclined solar panel basin solar still in passive and active mode. *Solar Energy, 169,* 206–216.
Murugavel, K. K., Anburaj, P., Hanson, R. S., & Elango, T. (2013). Progresses in inclined type solar stills. *Renewable and Sustainable Energy Reviews, 20,* 364–377.
Nagarajan, P. K., El-Agouz, S. A., DG, H. S., Edwin, M., Madhu, B., Sathyamurthy, R., et al. (2017). Analysis of an inclined solar still with baffles for improving the yield of fresh water. *Process Safety and Environmental Protection, 105,* 326–337.
Nayi, K. H., & Modi, K. V. (2018). Pyramid solar still: A comprehensive review. *Renewable and Sustainable Energy Reviews, 81,* 136–148.
Omara, Z. M., Kabeel, A. E., & Younes, M. M. (2013). Enhancing the stepped solar still performance using internal reflectors. *Desalination, 314,* 67–72.
Omara, Z. M., Kabeel, A. E., & Younes, M. M. (2014). Enhancing the stepped solar still performance using internal and external reflectors. *Energy Conversion and Management, 78,* 876–881.
Panchal, H., Taamneh, Y., Sathyamurthy, R., Kabeel, A. E., El-Agouz, S. A., Kumar, P. N., et al. (2017). Economic and exergy investigation of triangular pyramid solar still integrated to inclined solar still with baffles. *International Journal of Ambient Energy*. https://doi.org/10.1080/01430750.2017.1422143.
Praveen Kumar, B., Winston, D. P., Pounraj, P., Manokar, A. M., Sathyamurthy, R., & Kabeel, A. E. (2017). Experimental investigation on hybrid PV/T active solar still with effective heating and cover cooling method. *Desalination*. https://doi.org/10.1016/j.desal.2017.11.007.
Riahi, A., Wan Yusof, K., Mahinder Singh, B. S., Isa, M. H., Olisa, E., & Munni Zahari, N. A. (2015). Sustainable potable water production using a solar still with photovoltaic modules-AC heater. *Desalination and Water Treatment, 57,* 14929–14944. https://doi.org/10.1080/19443994.2015.1070285.
Saeedi, F., Sarhaddi, F., & Behzadmehr, A. (2015). Optimization of a PV/T (photovoltaic/thermal) active solar still. *Energy, 87,* 142–152.
Saini, V., Tiwari, S., & Tiwari, G. N. (2017). Environ economic analysis of various types of photovoltaic technologies integrated with greenhouse solar drying system. *Journal of Cleaner Production, 156,* 30–40.
Sathyamurthy, R., Nagarajan, P. K., El-Agouz, S. A., Jaiganesh, V., & Khanna, P. S. (2015). Experimental investigation on a semi-circular trough-absorber solar still with baffles for fresh water production. *Energy Conversion and Management, 97,* 235–242.
Sathyamurthy, R., Samuel, D. H., & Nagarajan, P. K. (2016). Theoretical analysis of inclined solar still with baffle plates for improving the fresh water yield. *Process Safety and Environmental Protection, 101,* 93–107.
Singh, D. B., & Tiwari, G. N. (2017a). Enhancement in energy metrics of double slope solar still by incorporating N identical PVT collectors. *Solar Energy, 143,* 142–161.
Singh, D. B., & Tiwari, G. N. (2017b). Performance analysis of basin type solar stills integrated with N identical photovoltaic thermal (PVT) compound parabolic concentrator (CPC) collectors: A comparative study. *Solar Energy, 142,* 144–158.

Singh, D. B., Tiwari, G. N., Al-Helal, I. M., Dwivedi, V. K., & Yadav, J. K. (2016a). Effect of energy matrices on life cycle cost analysis of passive solar stills. *Solar Energy, 134,* 9–22.
Singh, D. B., Yadav, J. K., Dwivedi, V. K., Kumar, S., Tiwari, G. N., & Al-Helal, I. M. (2016b). Experimental studies of active solar still integrated with two hybrid PVT collectors. *Solar Energy, 130,* 207–223.
Singh, D. B., Yadav, J. K., Dwivedi, V. K., Kumar, S., Tiwari, G. N., & Al-Helal, I. M. (2016c). Experimental studies of active solar still integrated with two hybrid PVT collectors. *Solar Energy, 130,* 207–223.
Tanaka, H. (2011). Tilted wick solar still with flat plate bottom reflector. *Desalination, 273*(2), 405–413.
Tanaka, H. (2013). Optimum inclination of still and bottom reflector for tilted wick solar still with flat plate bottom reflector. *Desalination and Water Treatment, 51*(34–36), 6482–6489.
Tanaka, H., & Nakatake, Y. (2007). Improvement of the tilted wick solar still by using a flat plate reflector. *Desalination, 216*(1–3), 139–146.
Tiwari, G. N., Yadav, J. K., Singh, D. B., Al-Helal, I. M., & Abdel-Ghany, A. M. (2015). Exergoeconomic and enviroeconomic analyses of partially covered photovoltaic flat plate collector active solar distillation system. *Desalination, 367,* 186–196.
Velmurugan, V., Kumar, K. N., Haq, T. N., & Srithar, K. (2009). Performance analysis in stepped solar still for effluent desalination. *Energy, 34*(9), 1179–1186.
Yari, M., Mazareh, A. E., & Mehr, A. S. (2016). A novel cogeneration system for sustainable water and power production by integration of a solar still and PV module. *Desalination, 398,* 1–11.

Affiliations

A. Muthu Manokar[1] · M. Vimala[2] · Ravishankar Sathyamurthy[3,4] · A. E. Kabeel[4] · D. Prince Winston[5] · Ali J. Chamkha[6]

1 Department of Mechanical Engineering, B.S. Abdur Rahman Crescent Institute of Science and Technology, Chennai 600 048, India

2 Department of Electrical and Electronics Engineering, R.M.K. Engineering College, Chennai 601 206, India

3 Department of Automobile Engineering, Hindustan Institute of Technology and Science, Chennai 603 103, Tamil Nadu, India

4 Mechanical Power Engineering Department, Faculty of Engineering, Tanta University, Tanta, Egypt

5 Department of Electrical and Electronics Engineering, Kamaraj College of Engineering and Technology, Virudhunagar 626 001, India

6 Mechanical Engineering Department, Prince Sultan Endowment for Energy and Environment, Prince Mohammad Bin Fahd University, Al-Khobar 31952, Saudi Arabia